On the Ejection of Dark Matter from Globular Clusters

T. Hurst and A. Zentner
Department of Physics and Astronomy, University of Pittsburgh, Pittsburgh, PA 15260, USA.
(Dated: August 29, 2016)

We investigate a mechanism for the removal of a DM halo from a GC. Through multi-body gravitational interactions, a DM particle can be ejected from the GC. However, we find that this mechanism is not efficient enough to eject a significant DM halo.

PACS numbers: PACS numbers go here. These are classification codes for your research. See `http://publish.aps.org/PACS/` for more info.

I. INTRODUCTION

In the ΛCDM paradigm, Dark Matter is the first matter constituent to collapse, forming Dark Matter halos which serve as the seeds for galaxy formation. Progressively larger structures are built through the mergers of halos. This hierarchical structure formation is predicted by theory and is seen in N-body simulations, as well as observed in the structure of galaxies and galaxy clusters.

One seeming exception to this scenario are Globular Clusters (GC). Reference [1] was the first to propose that GCs form in extended Dark Matter halos. However, observations of many GCs reveal thin tidal tails which N-body simulations predict should not form if they possess halos. Moreover recent studies of several GCs indicate that the ratio of the mass in Dark Matter to stars in several GCs $M_{\rm DM}/M_* \lesssim 1$ [2–7] and is potentially $\lesssim 10^{-2}$ if the Dark Matter is a low mass ($m_\chi \sim 10\,{\rm GeV}$) weakly interacting particle [8].

It is now generally thought GCs formed in gas compressed by shocks [9, 10]. However, the formation scenarios of GCs remain controversial in part because of the complex abundance patterns measured in stars. These observations indicate that GCs must have been much more massive in the past in order to retain significant amounts of heavy elements that would have been ejected by supernovae [11–13]. As pointed out in Reference [6] this formation scenario is further complicated by the existence of nuclear star clusters, which demonstrates that at least some GC-like systems form in Dark Matter halos (e.g. [14–17]).

Though they seemingly do not possess Dark Matter halos today, GCs could have had them in the past and subsequently lost their Dark Matter. One mechanism invoked for the removal of the halo is tidal stripping by the galaxy [18, 19]. While, the majority of the Galactic Globular Clusters (GGC) orbit within strong tidal fields there does exist a population of isolated GCs with galactocentric distances $r_{gc} > 70\,{\rm kpc}$ that should not have lost their halos through tidal interactions. Two such GCs are NGC 2419 ($r_{gc} = 89.9\,{\rm kpc}$) and MGC1, which at $\sim 200\,{\rm kpc}$ from M31 is the most isolated cluster in the local group [6, 20, 21]. Observations of both these cluster indicate that $M_{\rm DM}/M_* \lesssim 1$ [6, 7].

In this paper we investigate an additional mechanism by which GCs could eject Dark Matter halos: through multi-body gravitational interactions. In a close encounter with a star, a Dark Matter particle can be accelerated above the escape speed of the GC and be ejected. In principle, Dark Matter can also evaporate by slowly building up speed through multiple interactions. However, this mechanism is not efficient in GCs because particles with velocities near the escape speed spend most of their time near the outskirts of the GC and therefore, rarely experience an encounter with a star [22].

In this paper we will investigate the escape rate of Dark Matter particles from a spherically symmetric stellar system in order to ascertain the viability of the ejection scenario. As the interaction is gravitational, we shall not trouble ourselves with the details of the Dark Matter particle. The only assumption we make of the Dark Matter particle is that its mass is significantly less than the mass of a typical star.

The remainder of the paper is organized as follows: in §II we present the details of the calculation of the escape rate of Dark Matter particles from an isolated, spherical stellar system. In §III we present our results and in §IV we discuss our conclusions.

II. METHODS

Our calculation will follow the approach of a pair of classic papers by Hénon (Refs [22, 23] henceforth Papers 1 & 2 respectively). As in Paper 2, we begin with the assumption that the Dark Matter and stellar distributions are spherically symmetric and that the particle velocities are isotropic. Then, the number of Dark Matter particles in a

phase space volume element $\mathrm{d}^3r\mathrm{d}^3v$ is

$$(4\pi)^2 r^2 v^2 f(r,v)\mathrm{d}r\mathrm{d}v, \tag{1}$$

where $f(r,v)$ is the Dark Matter distribution function. Similarly, if the stellar distribution function is $g(r,v',m')$ then the number of stars in the volume element $\mathrm{d}^3r\mathrm{d}^3v'\mathrm{d}m'$ is

$$(4\pi)^2 r^2 v'^2 g(r,v',m')\mathrm{d}r\mathrm{d}v'\mathrm{d}m'. \tag{2}$$

Consider a Dark Matter particle of mass m_χ and coordinates (r,v). According to Paper 1 the probability that a particle will experience an encounter that takes it from a velocity $\vec{v} \to \vec{v} + \vec{e}$ is

$$P = 8\pi \mathrm{G}^2 \mathrm{d}t \frac{\mathrm{d}^3 e}{e^5} \int_0^\infty m'^2 \,\mathrm{d}m' \int_{v_0'}^\infty g(r,v',m') v' \,\mathrm{d}v', \tag{3}$$

where $v_0' = \frac{1}{e}|\vec{v}\cdot\vec{e} + \frac{m_\chi + m'}{2m'}e^2|$ and G is Newton's constant. The lower limit v_0' can be thought of as a statement of conservation of momentum. The relative velocity of the Dark Matter particle and star is unchanged in the encounter. It is only the velocity with respect to a thrid body, the GC as a whole in this case, that is changed.

As stated in §I, the one assumption of the Dark Matter particle we make is that $m_\chi \ll m'$ so

$$\begin{aligned} v_0' &= \frac{1}{e}|\vec{v}\cdot\vec{e} + \frac{e^2}{2}| \\ &= |v\cos\delta + \frac{e}{2}|. \end{aligned} \tag{4}$$

The particle will escape if

$$|\vec{v} + \vec{e}| \geq v_\mathrm{e}(r), \tag{5}$$

where $v_\mathrm{e}(r)$ is the local escape velocity. In the remainder of the paper we will denote the local escape velocity simply as v_e. Using the notation of Paper 2, let e, δ, φ be a set of spherical coordinates for the kick velocity $\vec{e}$. Then from Equation (5), the condition for escape is

$$v^2 + e^2 + 2ve\cos\delta \geq v_\mathrm{e}^2. \tag{6}$$

Then we can write the probability that the Dark Matter particle will escape in a time $\mathrm{d}t$ as:

$$Q = 8\pi \mathrm{G}^2 \mathrm{d}t \int_0^\infty m'^2 \,\mathrm{d}m' \int_{v_0'}^\infty g(r,v',m') v' \,\mathrm{d}v' \int_0^{2\pi} \mathrm{d}\varphi \int \sin\delta \,\mathrm{d}\delta \int e^{-3} \,\mathrm{d}e. \tag{7}$$

For a bound Dark Matter particle it must be the case that $v < v_\mathrm{e}$, then from (6)

$$v_\mathrm{e}^2 \leq v^2 + e^2 + 2ve\cos\delta \leq v_\mathrm{e}^2 + e^2 + 2ve\cos\delta, \tag{8}$$

therefore,

$$v\cos\delta \geq \frac{-e}{2}. \tag{9}$$

Hence, we can drop the absolute value in (4). Now,

$$Q = 16\pi^2 \mathrm{G}^2 \mathrm{d}t \int_0^\infty m'^2 \,\mathrm{d}m' \int_{v_0'}^\infty g(r,v',m') v' \,\mathrm{d}v' \int e^{-3} \,\mathrm{d}e \int \mathrm{d}\cos\delta, \tag{10}$$

where integration should satisfy:

$$-1 \leq \cos\delta \leq 1 \tag{11}$$

$$0 \leq e \tag{12}$$

$$v^2 + e^2 + 2ve\cos\delta \geq v_\mathrm{e}^2 \tag{13}$$

$$v\cos\delta + \frac{e}{2} \leq v' < v_{\rm e}. \tag{14}$$

To find the escape rate, we now integrate over the position and velocity of the Dark Matter particle. Let N_χ be the number of Dark Matter particles in the cluster,

$$N_\chi = \int_0^\infty 4\pi r^2\,{\rm d}r \int_0^{v_{\rm e}} 4\pi v^2 f(r,v)\,{\rm d}v \int_0^\infty N_\chi(m)\,{\rm d}m, \tag{15}$$

with $f(r,v)$ normalized to 1 and $N_\chi(m) = N_\chi\delta(m-m_\chi)$ assuming the halo is composed of a single Dark Matter constituent. Then the specific escape rate is

$$\begin{aligned}\left|\frac{1}{N_\chi}\frac{\partial N_\chi}{\partial t}\right| &= \int_0^\infty 4\pi r^2\,{\rm d}r \int_0^{v_{\rm e}} 4\pi v^2 \frac{Q}{{\rm d}t} f(r,v)\,{\rm d}v \\ &= 256\pi^4 {\rm G}^2 \int_0^\infty r^2\,{\rm d}r \int_0^{v_{\rm e}} v^2 f(r,v)\,{\rm d}v \\ &\times \int_0^\infty m'^2\,{\rm d}m' \int_{v'_0}^\infty g(r,v',m')v'\,{\rm d}v' \int e^{-3}\,{\rm d}e \int {\rm d}\cos\delta,\end{aligned} \tag{16}$$

with the limits in Equations(11)-(14) satisfied and where we have taken the magnitude since $\frac{\partial N_\chi}{\partial t}$ is negative. If the magnitude of the specific escape rate is greater than τ^{-1} with τ the age of the Universe, then a typical Dark Matter particle will have been ejected from the halo. It is therefore likely that the GC would have dissipated its halo by the present time *via* this mechanism. We normalized Equation (15) to N_χ rather than 1 to make this point explicit.

As noted in Paper 2, this expression looks quite intractable, but the integrals in e and δ can in fact be calculated analytically. Keeping with the notation of Paper 2 let

$$S = \int e^{-3}\,{\rm d}e \int {\rm d}\cos\delta, \tag{17}$$

and let $C = \cos\delta$. From (13)

$$C \geq \frac{v_{\rm e}^2 - v^2 - e^2}{2ve} = C_1, \tag{18}$$

from (14)

$$C \leq \frac{v' - \frac{e}{2}}{v} = C_2, \tag{19}$$

and from (11)

$$C_3 = -1 \leq C \leq 1 = C_4. \tag{20}$$

In order for S to be non-zero we must have that $C_1 < C_4, C_1 < C_2, C_3 < C_4$, and $C_3 < C_2$. Now $C_3 < C_4$ trivially. $C_1 < C_4$ requires that,

$$e > v_{\rm e} - v = e_1, \tag{21}$$

which is stronger than (12). $C_1 < C_2$ requires that,

$$e > \frac{v_{\rm e}^2 - v^2}{2v'} = e_2, \tag{22}$$

which is again stronger than (12). And $C_3 < C_2$ requires that,

$$e < 2(v' + v) = e_3, \tag{23}$$

which further restricts (12). C_3 will be the lower limit of the ${\rm d}C$ integral when $C_1 < C_3$ or when

$$e > v + v_{\rm e} = e_4, \tag{24}$$

and C_2 will be the upper limit when $C_2 < C_4$ or when

$$e > 2(v' - v) = e_5. \tag{25}$$

Thus, in order to determine the limits of the integrals in S, we must consider the order of e_1, e_2, e_3, e_4, and e_5. Elementary calculations show that

$$\begin{aligned} v' &\geq \frac{1}{2}(v_\mathrm{e} - 3v) = v_1' \Rightarrow e_1 \leq e_3 \\ v' &\geq \frac{1}{2}(v_\mathrm{e} - v) = v_2' \Rightarrow e_2 \leq e_3, e_2 \leq e_4, e_4 \leq e_3 \\ v' &\geq \frac{1}{2}(v_\mathrm{e} + v) = v_3' \Rightarrow e_2 \leq e_1, e_1 \leq e_5, e_2 \leq e_5 \\ v' &\geq \frac{1}{2}(v_\mathrm{e} + 3v) = v_4' \Rightarrow e_4 \leq e_5 \end{aligned} \tag{26}$$

and it is always true that $e_1 \leq e_4$ and $e_5 \leq e_3$. These relations divide the v-v' plane into 5 regions A, B, C, D, and E (see Figure 1). In region A,

$$e_5 \leq e_1 \leq e_2 \leq e_4 \leq e_3. \tag{27}$$

Thus in region A we have,

$$\begin{aligned} S_\mathrm{A} &= \int_{e_2}^{e_4} e^{-3}\,\mathrm{d}e \int_{C_1}^{C_2} \mathrm{d}C + \int_{e_4}^{e_3} e^{-3}\,\mathrm{d}e \int_{C_3}^{C_2} \mathrm{d}C \\ &= \frac{2v'^3}{3v(v_\mathrm{e}^2 - v^2)^2} + \frac{1}{8v(v' + v)} - \frac{2v_\mathrm{e} + v}{6v(v_\mathrm{e} + v)^2}. \end{aligned} \tag{28}$$

In region B,

$$e_2 \leq e_1 \leq e_5 \leq e_4 \leq e_3. \tag{29}$$

Hence,

$$\begin{aligned} S_\mathrm{B} &= \int_{e_1}^{e_5} e^{-3}\,\mathrm{d}e \int_{C_1}^{C_4} \mathrm{d}C + \int_{e_5}^{e_4} e^{-3}\,\mathrm{d}e \int_{C_1}^{C_2} \mathrm{d}C + \int_{e_4}^{e_3} e^{-3}\,\mathrm{d}e \int_{C_3}^{C_2} \mathrm{d}C \\ &= \frac{3v_\mathrm{e}^2 - v^2}{3(v_\mathrm{e} - v)^2(v_\mathrm{e} + v)^2} - \frac{1}{4(v'^2 - v^2)}. \end{aligned} \tag{30}$$

In region C,

$$e_2 \leq e_1 \leq e_4 \leq e_5 \leq e_3. \tag{31}$$

Hence,

$$\begin{aligned} S_\mathrm{C} &= \int_{e_1}^{e_4} e^{-3}\,\mathrm{d}e \int_{C_1}^{C_4} \mathrm{d}C + \int_{e_4}^{e_5} e^{-3}\,\mathrm{d}e \int_{C_3}^{C_4} \mathrm{d}C + \int_{e_5}^{e_3} e^{-3}\,\mathrm{d}e \int_{C_3}^{C_2} \mathrm{d}C \\ &= \frac{3v_\mathrm{e}^2 - v^2}{3(v_\mathrm{e} - v)^2(v_\mathrm{e} + v)^2} - \frac{1}{4(v'^2 - v^2)} \\ &= S_\mathrm{B}. \end{aligned} \tag{32}$$

In region D,

$$e_5 \leq e_3 \leq e_1 \leq e_4 \leq e_2. \tag{33}$$

Here we can not simultaneously satisfy $e > e_1, e > e_2$, and $e < e_3$, thus region D is forbidden. In region E,

$$e_5 \leq e_1 \leq e_3 \leq e_4 \leq e_2. \tag{34}$$

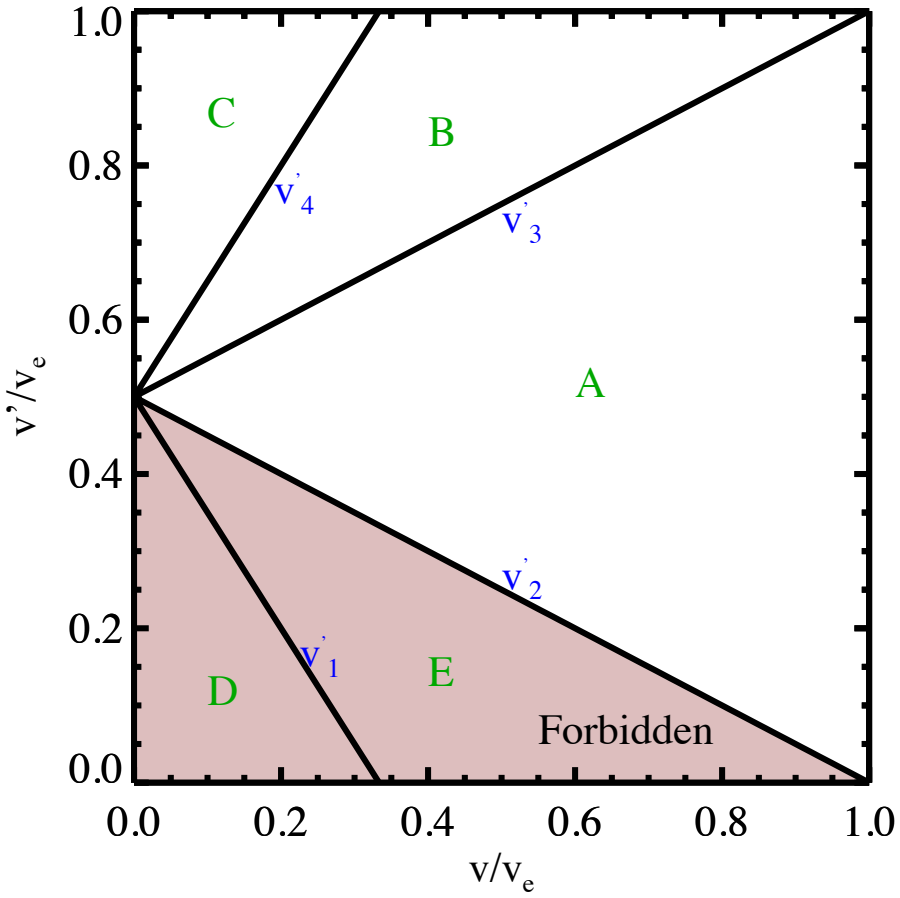

FIG. 1: The integration regions over the kick velocity $\vec{e}$. The shading denotes the fact that regions D & E are forbidden because we cannot simultaneously satisfy all of the required inequalities in Eqs. (11-14).

So region E is forbidden for the same reason as D. Then Eq. (16) becomes,

$$\begin{aligned}\left|\frac{1}{N_\chi}\frac{\partial N_\chi}{\partial t}\right| = 256\pi^4 \mathrm{G}^2 \int_0^\infty r^2\,\mathrm{d}r \int_0^\infty m'^2\,\mathrm{d}m' \\ \times \Bigg\{ \int_0^{v_\mathrm{e}} v^2 f(r,v)\,\mathrm{d}v \int_{v'_2}^{v'_3} v' S_\mathrm{A} g(r,v',m')\,\mathrm{d}v' \\ + \int_0^{v_\mathrm{e}/3} v^2 f(r,v)\,\mathrm{d}v \int_{v'_3}^{v'_4} v' S_\mathrm{B} g(r,v',m')\,\mathrm{d}v' \\ + \int_{v_\mathrm{e}/3}^{v_\mathrm{e}} v^2 f(r,v)\,\mathrm{d}v \int_{v'_3}^{v_\mathrm{e}} v' S_\mathrm{B} g(r,v',m')\,\mathrm{d}v' \\ + \int_0^{v_\mathrm{e}/3} v^2 f(r,v)\,\mathrm{d}v \int_{v'_4}^{v_\mathrm{e}} v' S_\mathrm{B} g(r,v',m')\,\mathrm{d}v' \Bigg\}.\end{aligned} \tag{35}$$

In order to proceed further we must specify the stellar and Dark Matter distribution functions. As in Paper 2, we take for the stellar component a Plummer model

$$\rho_*(r) = \frac{3M_*}{4\pi}\frac{r_0^2}{(r^2+r_0^2)^{5/2}}, \tag{36}$$

where r_0 is the half-mass radius of the GC. As there is little guidance on what the distribution function of Dark

Matter in a GC might be, we will also use a Plummer model for the Dark Matter

$$\rho_\chi(r) = \frac{3M_{\rm DM}}{4\pi}\frac{r_\chi^2}{(r^2+r_\chi^2)^{5/2}}, \tag{37}$$

where r_χ is the half-mass radius of the Dark Matter halo. We choose the Plummer model for the Dark Matter in part because it has some nice mathematical properties that make it a convenient choice. As we shall see below, the Plummer distribution function allows us to separate the radial and velocity integrals. There is also a factor of $\left(\frac{v_{\rm e}^2-v^2}{2}\right)^{7/2}$ in the distribution function which cancels out the divergence of $(v_{\rm e}^2-v^2)^{-2}$ in $S_{\rm A}$. Moreover, the Plummer model is reasonably realistic for GCs [22] and is similar to the structures of simulated Dark Matter halos and elliptical galaxies. One shortcoming of the Plummer model is that it lacks mass segregation which is known to occur (e.g. [24]). This in turn implies that velocities are uncorrelated, but the error is small and there is no known analytical cluster model with mass segregation [22].

Now the gravitational potential is

$$\phi(r) = \frac{-GM_*}{\left(r^2+r_0^2\right)^{1/2}} + \frac{-GM_{\rm DM}}{\left(r^2+r_\chi^2\right)^{1/2}}. \tag{38}$$

In general the half-mass radii of the 2 components need not be the same. If $r_\chi \neq r_0$ the analytic expressions needed to derive the distribution function become cumbersome and we treat this case numerically. Due to the assumption of isotropy, the distribution function depends only on the magnitude of the velocity, or equivalently the kinetic energy. Figure 2 shows the distribution function $f(\varepsilon)$ as a function of the magnitude of the specific energy $\left(\varepsilon = \frac{1}{2}[v_{\rm e}^2 - v^2]\right)$ for a GC with $M_* = 2\times10^6\,{\rm M}_\odot,\ r_0 = 10\,{\rm pc}$. The solid line is the standard Plummer model in the case that $r_\chi = r_0$. The dashed green line shows the numerical result for this case, which is in agreement with the analytic case. The dotted line shows the distribution function in the case that $r_\chi = r_0/10$ while the dot-dashed line shows the case where $r_\chi = 10r_0$. The inset is a zoom in of the latter case, which shows the feature at $\varepsilon \approx 150\,({\rm km/s})^2$. Since ε is inversely proportional to r, when $r_\chi = r_0/10$ we expect that most of the Dark Matter should be at large ε (small r). The flat part of the distribution function near $\varepsilon = 2000\,({\rm km/s})^2$ is the transition from mostly stars at large r to stars and Dark Matter at $r \sim r_0/10$. The distribution function is also pushed to higher energies as more mass is concentrated in the center, increasing the orbital velocities in that region. The oppositie is true for the case $r_\chi = 10r_0$.

In the case that $r_0 = r_\chi$ we will have the standard Plummer distribution,

$$f(r,v) = \frac{24\sqrt{2}}{7\pi^3 r_0^3\psi_0^5}\left(\frac{v_{\rm e}^2-v^2}{2}\right)^{\frac{7}{2}} \tag{39}$$

where $\psi_0 = \frac{GM}{r_0}$ with $M = M_* + M_{\rm DM}$ the total mass of the cluster and $E = \frac{-3\pi\psi_0^2 r_0}{64{\rm G}}$ its energy.

With the choice that $r_\chi = r_0$ we have that

$$\begin{aligned} v_{\rm e} &= \sqrt{2\psi} \\ &= \frac{(2\psi_0)^{1/2}}{\left(1+\frac{r^2}{r_0^2}\right)^{1/4}}, \end{aligned} \tag{40}$$

where we have defined $\psi(r) = -\phi(r)$. Defining the stellar mass spectrum $N_*(m){\rm d}m$ as the number of stars in the mass interval $m \to m + {\rm d}m$, we have that $g(r,v',m') = f(r,v')N_*(m')$. Then Equation (35) becomes

$$\begin{aligned} \left|\frac{1}{N_\chi}\frac{\partial N_\chi}{\partial t}\right| = \frac{2304{\rm G}^2}{49\pi^2 r_0^6\psi_0^{10}} \int_0^{R_{\rm vir}} r^2\,{\rm d}r \int_0^\infty N_*(m')m'^2\,{\rm d}m' \\ \times\Bigg\{ \int_0^{v_{\rm e}} v^2(v_{\rm e}^2-v^2)^{\frac{7}{2}}\,{\rm d}v \int_{v_2'}^{v_3'} v' S_{\rm A}(v_{\rm e}^2-v'^2)^{7/2}\,{\rm d}v' \\ + \int_0^{v_{\rm e}/3} v^2(v_{\rm e}^2-v^2)^{\frac{7}{2}}\,{\rm d}v \int_{v_3'}^{v_4'} v' S_{\rm B}(v_{\rm e}^2-v'^2)^{7/2}\,{\rm d}v' \\ + \int_{v_{\rm e}/3}^{v_{\rm e}} v^2(v_{\rm e}^2-v^2)^{\frac{7}{2}}\,{\rm d}v \int_{v_3'}^{v_{\rm e}} v' S_{\rm B}(v_{\rm e}^2-v'^2)^{7/2}\,{\rm d}v' \\ + \int_0^{v_{\rm e}/3} v^2(v_{\rm e}^2-v^2)^{\frac{7}{2}}\,{\rm d}v \int_{v_4'}^{v_{\rm e}} v' S_{\rm B}(v_{\rm e}^2-v'^2)^{7/2}\,{\rm d}v' \Bigg\}. \end{aligned} \tag{41}$$

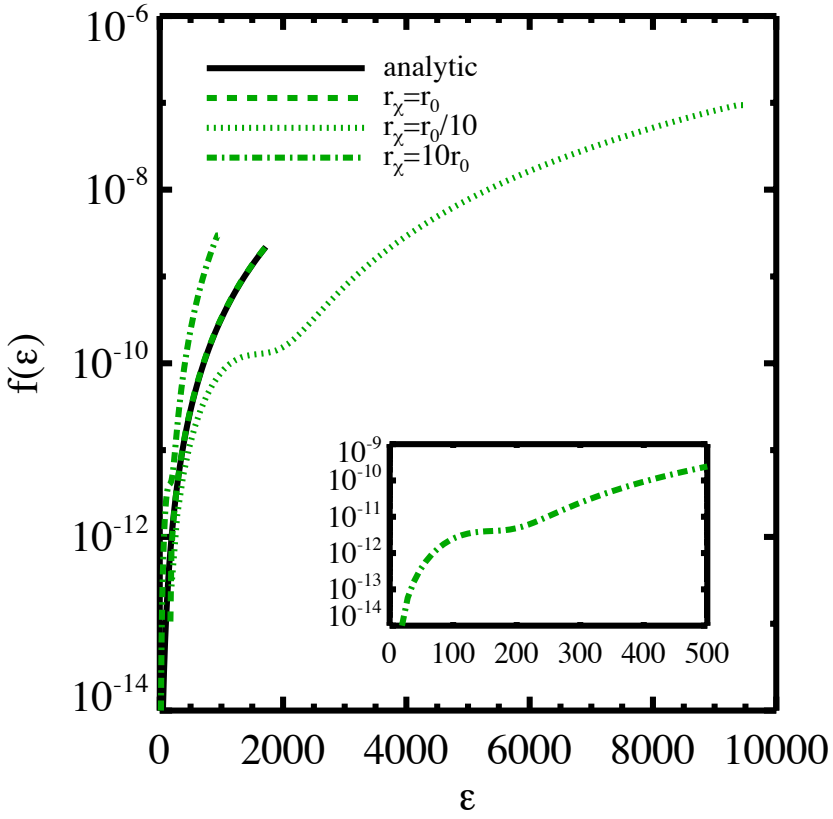

FIG. 2: The distribution function $f(\varepsilon)$ as a function of the magnitude of the specific energy $\left(\varepsilon = \frac{1}{2}[v_e^2 - v^2]\right)$. The solid line is the standard Plummer model in the case that $r_\chi = r_0$. The dashed green line shows the numerical result for this case which is in agreement with the analytic case. The dotted line shows the distribution function in the case that $r_\chi = r_0/10$ while the dot-dashed line shows the case where $r_\chi = 10r_0$. The inset is a zoom in of the latter case, which shows the feature at $\varepsilon \approx 150$.

where the virial radius $R_{\rm vir}$ of the Dark Matter halo is chosen to be suitably large ($\sim 10r_0$)such that the integrals in Equation (41) are all converged.

Continuing the approach of Paper 2, we now define new variables:

$$x = v/v_e, \qquad x' = v'/v_e. \tag{42}$$

Then we can remove v_e from the integrals over v and v' and perform those integrals separately from the radial integral. It is proven in Appendix II of Paper 2 that the Plummer model is the only steady state distribution for which this

separation is possible. Then Equation (41) becomes

$$\begin{aligned}\left|\frac{1}{N_\chi}\frac{\partial N_\chi}{\partial t}\right| = \frac{2304\mathrm{G}^2}{49 r_0^6 \psi_0^{10}} \int_0^{R_{\rm vir}} v_{\rm e}^{17} r^2 \,\mathrm{d}r \int_0^\infty N_*(m') m'^2 \,\mathrm{d}m' \\ \times \Bigg\{ \int_0^1 x^2(1-x^2)^{\frac{7}{2}} \,\mathrm{d}x \int_{x_2'}^{x_3'} x' S_{\rm A}'(1-x'^2)^{7/2} \,\mathrm{d}x' \\ + \int_0^{1/3} x^2(1-x^2)^{\frac{7}{2}} \,\mathrm{d}x \int_{x_3'}^{x_4'} x' S_{\rm B}'(1-x'^2)^{7/2} \,\mathrm{d}x' \\ + \int_{1/3}^1 x^2(1-x^2)^{\frac{7}{2}} \,\mathrm{d}x \int_{x_3'}^1 x' S_{\rm B}'(1-x'^2)^{7/2} \,\mathrm{d}x' \\ + \int_0^{1/3} x^2(1-x^2)^{\frac{7}{2}} \,\mathrm{d}x \int_{x_4'}^1 x' S_{\rm B}'(1-x'^2)^{7/2} \,\mathrm{d}x' \Bigg\},\end{aligned} \tag{43}$$

where

$$\begin{aligned} x_2' &= \frac{1}{2}(1-x) \\ x_3' &= \frac{1}{2}(1+x) \\ x_4' &= \frac{1}{2}(1+3x), \end{aligned} \tag{44}$$

and the $'$ in S_i' denotes the fact that it is now a function of x and x' with $v_{\rm e}$ factored out.

Let us now choose a particular stellar mass spectrum. We begin with the Initial Mass Function (IMF) from Reference [25]. All of the GGCs should have ages of order ~ 10 Gyr, meaning that their Main Sequence (MS) turnoffs should be at approximately $1\,\mathrm{M}_\odot$. Therefore, in order to obtain a crude approximation of the present day stellar mass spectrum, we simply cut off the IMF at $1\,\mathrm{M}_\odot$ (see Figure 3). Note that this is highly conservative as stellar remnants such as Neutron Stars, White Dwarfs, and Black Holes as well as any stars still on the Giant and Horizontal Branches should contribute to the escape rate. Furthermore, higher mass stars are given more weight in the integral over mass in Equation (43).

With this choice of stellar mass spectrum we have that

$$\int_0^\infty N_*(m') m'^2 \,\mathrm{d}m' = 0.18M. \tag{45}$$

III. RESULTS

In Figure 4 we consider the result of integrating Equation (43) numerically for different values of the ratio $M_{\rm DM}/M_*$ and compare these results to the GGCs (as well as the cluster MGC1 located in M31). Contours of the specific escape rate for GCs with $r_0 = r_\chi$ are shown with solid black lines. The red star represents MGC1, an isolated cluster orbiting M31, while the blue diamonds represent the isolated population of GGCs ($r_{gc} > 70$ kpc). As noted in §I, most of the GGCs could have lost their Dark Matter halos through tidal interactions with the Galaxy. We shall therefore pay particular attention to the most isolated GCs. GGCs that have been selected for further investigation in Figure 5 are marked with pink squares while the green triangles denote the remaining GGCs. The solid blue line is the location where the specific escape rate is $1/\tau$ with $\tau = 13.8$ Gyr the approximate age of the Universe [26]. GCs with escape rates comparable to or exceeding this limit should have ejected a significant portion of their Dark Matter halos. However, none of the clusters reach this limit regardless of the value of $M_{\rm DM}/M_*$. Note that the escape rate is no longer sensitive to the value of $M_{\rm DM}/M_*$ once this ratio has dropped below $\sim 10^{-2}$. We also note that more massive GCs have lower escape rates due to their higher escape speeds, while GCs which are larger in size have lower escape rates due to the decreased probability of experiencing an encounter at higher radii (see Figure 2).

In Figures 5 & 6 we consider the effect of varying r_χ with respect to r_0 while holding $M_{\rm DM}/M_* = 1$. We consider $r_\chi = 10 r_0$ which might correspond to an extended primordial halo as well as $r_\chi = 10^{-1} r_0$ which might correspond to a cluster which has had the outer part of its Dark Matter halo stripped by tidal interactions. The results are obtained by integrating Equation (35) with the appropriate numerically derived distribution functions (see Figure 2).

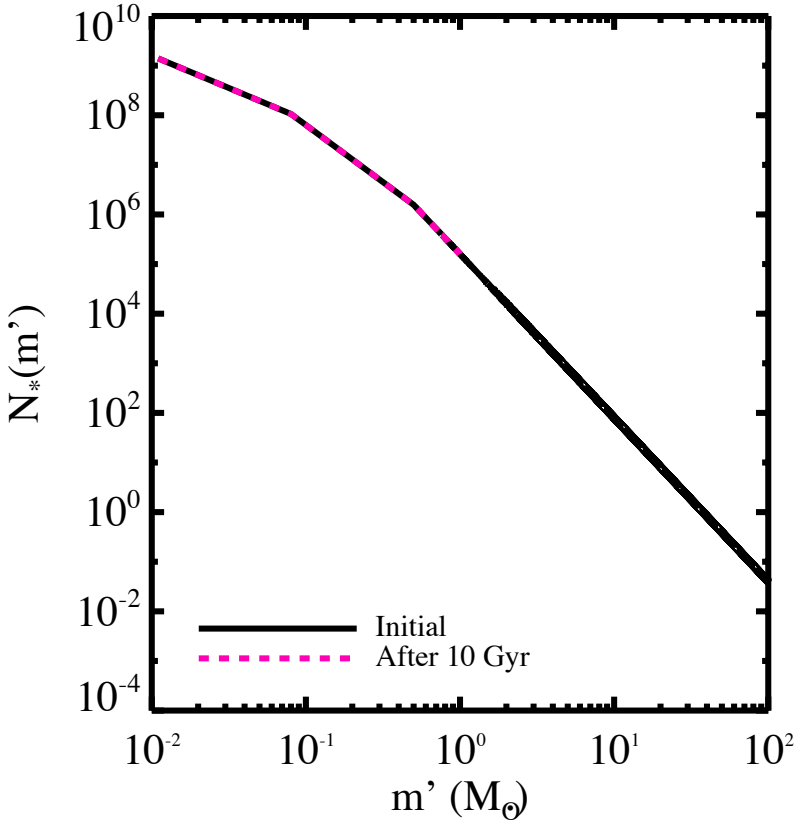

FIG. 3: The solid black line is the IMF from Ref. [25]. After 10 Gyr (the approximate age of a GGC) stars more massive than $1\,M_\odot$ will have left the MS. We therefore cut the IMF off at $1\,M_\odot$ in order to approximate the present day stellar mass spectrum. This is a highly conservative choice as the remnants of more massive stars and stars still on the Giant and Horizontal Branches should also contribute to the escape rate.

Note that for $r_\chi = 10r_0$, much of the Dark Matter exists beyond the stellar content of the GC and therefore never experiences a close encounter with a star. Thus we might normalize Equation (35) by the number of Dark Matter particles within the stellar content, rather than the total number of particles. Since we have taken the virial radius of the cluster to be $R_{\rm vir} = 10r_0$, exactly half the Dark Matter particles should be within $R_{\rm vir}$ in the case of an extended halo. Therefore we could multiply the results for $r_\chi = 10r_0$ by a factor of 2 in Figures 5 & 6.

We first consider, in Figure 5, the GCs that are marked with pink squares in Figure 4. The parameters for these clusters are summarized in Table I and span the full range of GGCs. Note that decreasing r_χ increases the escape rate. This result is perhaps counter intuitive as a smaller halo should have a deeper potential well which is correspondingly more difficult to escape from. However, in a smaller halo, the probability of experiencing an encounter is much higher, which explains the results. Of course, the opposite is true for larger halos. Though they are easier to escape from, the probability of encounter is decreased. Note, that for $M_{\rm DM}/M_* = 1$ the only halo which exceeds $1/\tau$ is that of Pal 1 in the case that $r_\chi = 10^{-1}r_0$. However, the escape rate can be increased by an additional half dex for smaller values of the ratio $M_{\rm DM}/M_*$. Fig 5 then indicates that clusters with $M_{\rm DM}/M_* \lesssim 10^{-2}$ and r_0 not more than a few parsecs, could have ejected a small remnant halo after the initial halo was tidally stripped. This also suggests that such clusters could have significantly dispersed the inner regions of their halos, even if their halos were larger.

In Figure 6 we consider the escape rates for the most isolated clusters in the Milky Way (and M31) which are marked with blue diamonds in Fig 4. The parameters for these clusters are summarized in Table II. Due to their large sizes ($r_0 > 10\,{\rm pc}$), these clusters all have escape rates far below $1/\tau$. This is further evidence against the formation of GCs in Dark Matter halos.

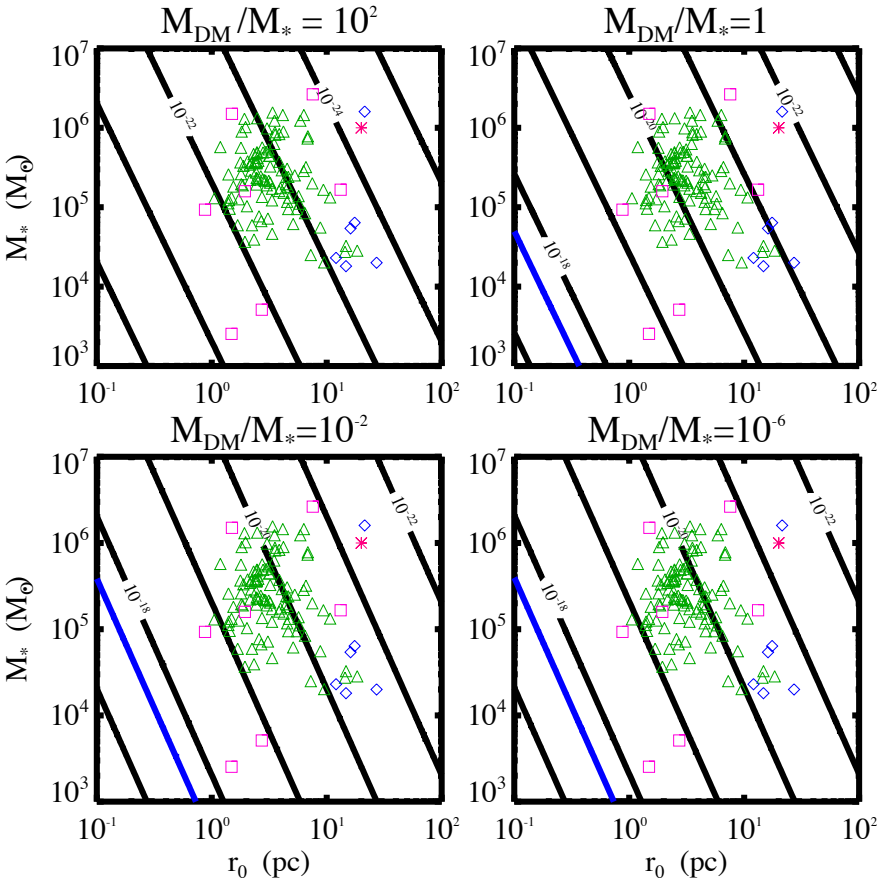

FIG. 4: Contours of the specific escape rate for GCs with $r_0 = r_\chi$. Each panel shows a different value of the ratio $M_{\rm DM}/M_*$. The red star represents MGC1, an isolated cluster orbiting M31, while the blue diamonds represent the isolated popluation of GGCs ($r_{gc} > 70$ kpc). These isolated GCs are further considered in Fig. 6. GGCs that have been selected for further investigation in Fig. 5 are marked with pink squares while the green triangles denote the remaining GGCs. The solid blue line is the location where the specific escape rate is $1/\tau$ with $\tau = 13.8$ Gyr the approximate age of the Universe [26]. GCs with escape rates comparable to or exceeding this limit should have ejected a significant portion of their DM halos. However, none of the clusters reach this limit regardless of the value of $M_{\rm DM}/M_*$, with the most massive halos having the lowest escape rates as expected.

GC	$M_*(\mathrm{M}_\odot)$	r_0 (pc)	$M_{\rm DM}/M_*$
Pal 1	2.54×10^3	1.49	—
Pal 13	5.12×10^3	2.72	—
NGC 5053	1.66×10^5	13.2	—
NGC 5139	2.64×10^6	7.56	—
NGC 6388	1.50×10^6	1.50	—
NGC 6397	1.59×10^5	1.94	$\lesssim 1$ [5]
NGC 6528	9.31×10^4	0.87	—

TABLE I: Parameters for the GCs in Figure 5 [20].

IV. CONCLUSIONS

GCs are peculiar systems in that they are the largest structures in the Universe not dominated by Dark Matter. Though they do not possess halos today, it is possible that they did in the past. One viable mechanism by which GCs can lose Dark Matter halos is through tidal interactions with the Galaxy. However, there exists a population of isolated GCs which should not have had their halos tidally stripped if they ever possessed them. Observations of 2 of these GCs (NGC 2419 & MGC1) indicate that they do not possess significant halos today ($M_{\rm DM} \lesssim M_*$ see Table II).

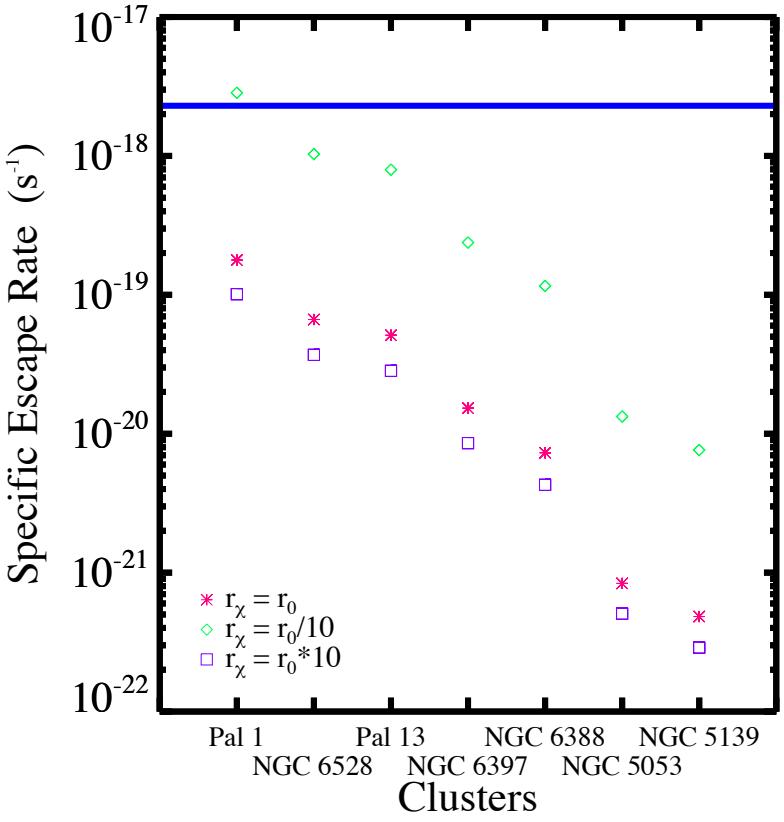

FIG. 5: Escape rates for several GGCs for different values of r_χ/r_0 under the assumption that $M_{\rm DM}/M_* = 1$. The solid blue line denotes $1/\tau$.

GC	$M_*(\mathrm{M}_\odot)$	r_0 (pc)	r_{gc} (kpc)	$M_{\rm DM}/M_*$
AM 1	1.81×10^4	14.7	124.6	—
Eridanus	2.30×10^4	12.1	95.0	—
Pal 3	6.38×10^4	17.5	95.7	—
Pal 4	5.41×10^4	16.1	111.2	—
NGC 2419	1.60×10^6	21.4	89.9	$\lesssim 1$ [6, 7]
Pal 14	2.00×10^4	27.1	71.6	—
MGC 1	1×10^6	20	200	$\lesssim 1$ [6]

TABLE II: Parameters for the isolated GCs in Figure 6 [20].

In this paper we have investigated an additional mechanism for the removal of Dark Matter from a GC: the ejection of Dark Matter by multi-body gravitational interactions. We have found that GCs could not have ejected a significant Dark Matter halo with one exception. GCs that are sufficiently small could have ejected a small remnant halo after the majority of the halo was tidally stripped. Our results cast further doubt on the formation of GCs in extended, massive Dark Matter halos.

In the context of WIMP astronomy, GCs remain interesting targets. As the stellar density of a GC is extremely high ($10^4 - 10^6\,\mathrm{stars/pc^3}$), even a subdominant Dark Matter halo could have a density several orders of magnitude greater than that of the Solar neighborhood $\rho_\chi \sim 0.4\,\mathrm{GeV/cm^3}$. Current limits on the mass of any hypothetical Dark Matter halo are of order the stellar mass of the cluster. Our results indicate that such a halo should persist to the present day. This would make the isolated GCs viable targets for the methods of §**??**.

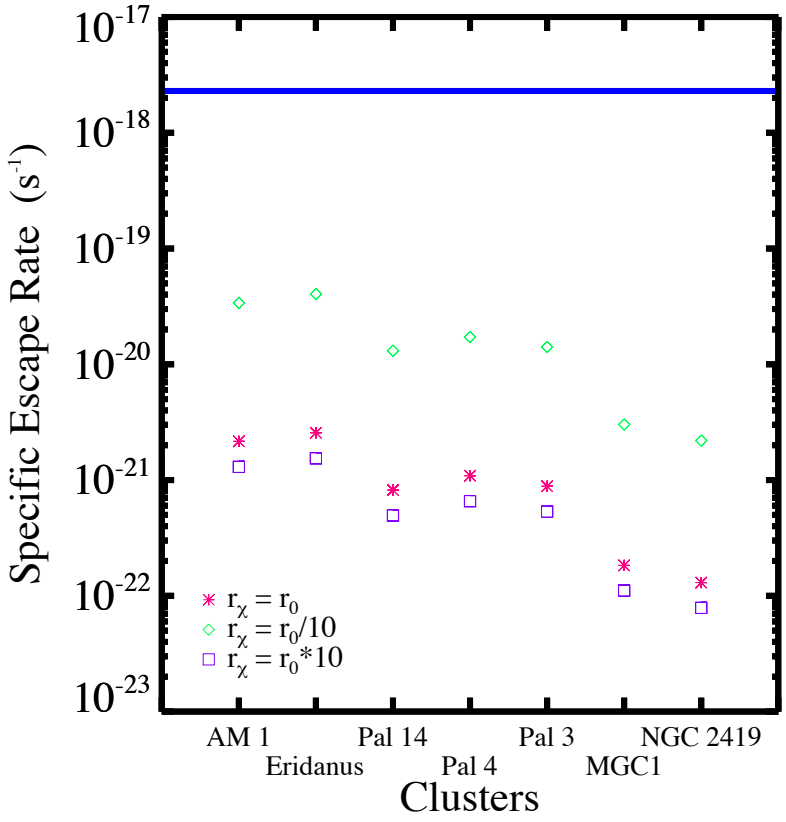

FIG. 6: Escape rates for the isolated GCs for different values of r_χ/r_0 under the assumption that $M_{\rm DM}/M_* = 1$. The solid blue line denotes $1/\tau$.

Acknowledgments

[1] P. J. E. Peebles, ApJ **277**, 470 (1984).
[2] C. J. Grillmair, K. C. Freeman, M. Irwin, and P. J. Quinn, AJ **109**, 2553 (1995), astro-ph/9502039.
[3] M. Odenkirchen, E. K. Grebel, W. Dehnen, H.-W. Rix, B. Yanny, H. J. Newberg, C. M. Rockosi, D. Martínez-Delgado, J. Brinkmann, and J. R. Pier, AJ **126**, 2385 (2003), astro-ph/0307446.
[4] B. Moore, ApJL **461**, L13 (1996), astro-ph/9511147.
[5] J. Shin, S. S. Kim, and Y.-W. Lee, Journal of Korean Astronomical Society **46**, 173 (2013).
[6] C. Conroy, A. Loeb, and D. N. Spergel, ApJ **741**, 72 (2011), 1010.5783.
[7] R. Ibata, C. Nipoti, A. Sollima, M. Bellazzini, S. C. Chapman, and E. Dalessandro, MNRAS **428**, 3648 (2013), 1210.7787.
[8] T. J. Hurst, A. R. Zentner, A. Natarajan, and C. Badenes, Phys Rev D **91**, 103514 (2015), 1410.3925.
[9] J. E. Gunn, in *Globular Clusters*, edited by D. Hanes and B. Madore (1980), p. 301.
[10] W. E. Harris and R. E. Pudritz, ApJ **429**, 177 (1994).
[11] R. Gratton, C. Sneden, and E. Carretta, ARAA **42**, 385 (2004).
[12] R. G. Gratton, E. Carretta, and A. Bragaglia, AAPR **20**, 50 (2012), 1201.6526.
[13] C. Conroy and D. N. Spergel, ApJ **726**, 36 (2011), 1005.4934.
[14] M. A. Taylor, T. H. Puzia, M. Gomez, and K. A. Woodley, Ap J **805**, 65 (2015), 1503.04198.
[15] T. Böker, M. Sarzi, D. E. McLaughlin, R. P. van der Marel, H.-W. Rix, L. C. Ho, and J. C. Shields, AJ **127**, 105 (2004), astro-ph/0309761.
[16] C. J. Walcher, R. P. van der Marel, D. McLaughlin, H.-W. Rix, T. Böker, N. Häring, L. C. Ho, M. Sarzi, and J. C. Shields, Ap J **618**, 237 (2005), astro-ph/0409216.

[17] C. J. Walcher, T. Böker, S. Charlot, L. C. Ho, H.-W. Rix, J. Rossa, J. C. Shields, and R. P. van der Marel, Ap J **649**, 692 (2006), astro-ph/0604138.
[18] V. Bromm and C. J. Clarke, ApJL **566**, L1 (2002), astro-ph/0201066.
[19] S. Mashchenko and A. Sills, ApJ **619**, 258 (2005), astro-ph/0409606.
[20] W. E. Harris, The Astronomical Journal **112**, 1487 (1996).
[21] A. D. Mackey, A. M. N. Ferguson, M. J. Irwin, N. F. Martin, A. P. Huxor, N. R. Tanvir, S. C. Chapman, R. A. Ibata, G. F. Lewis, and A. W. McConnachie, MNRAS **401**, 533 (2010), 0909.1456.
[22] M. Henon, Astronomy and Astrophysics **2**, 151 (1969).
[23] M. Hénon, Annales d'Astrophysique **23**, 467 (1960).
[24] S. J. Aarseth, MNRAS **132**, 35 (1966).
[25] P. Kroupa, MNRAS **322**, 231 (2001), astro-ph/0009005.
[26] Planck Collaboration, P. A. R. Ade, N. Aghanim, M. Arnaud, M. Ashdown, J. Aumont, C. Baccigalupi, A. J. Banday, R. B. Barreiro, J. G. Bartlett, et al., ArXiv e-prints (2015), 1502.01589.